ICAS 2020 SHANGHAI
International Council of the Aeronautical Sciences
32nd Congress of the International Council of the Aeronautical Sciences
September 6-10, 2021
Pudong Shangri-La, Shanghai, China

NUMERICAL SIMULATION OF LOCAL LONG SHALLOW CAVITY EFFECT ON THE STABILITY OF A HYPERSONIC BOUNDARY LAYER

Yang Jiaji[1], Zhang Yudong[1], Lv Peng[1] & Tiziano Pagliaroli[2]

[1]China Academy of Aerospace Aerodynamics, Beijing 100074, China
[2]Department of Economy, Università Niccolò Cusano, Via Don Carlo Gnocchi 3, Rome 00166, Italy

Abstract

The stability of a hypersonic boundary layer over a flat plate with the effect of a long shallow cavity investigated by spatial direct numerical simulation. Unsteady disturbance is introduced by a slot of periodic suction-blowing at the plate leading edge. The results indicate the stabilization effect is influenced by the frequency of the second mode. For all the cases studied, the cavity is located in the close downstream region of the synchronization point corresponding to the most dangerous frequency. With the depth of the cavity increases, the stabilization of second mode improved. But flow separation in the cavity reduces the stabilization effect.

Keywords: Hypersonic boundary layer, Boundary layer transition, Flow control, Second mode.

1. Introduction

In hypersonic boundary layer laminar to turbulent transition increases significantly the shear stress and heat flux. Therefore, the weight, complexity and cost of thermal protection system (TPS) of hypersonic vehicles can be reduced by delaying the laminar-turbulent transition. Transition is a multifold process that evolves in many different ways depending on numerous parameters of the mean flow and disturbances[1]. When freestream disturbances are small, for high-altitude flights with smooth surfaces under hypersonic flow, transition to turbulence occurs due to amplification of the unstable disturbances of the first and/or second mode[2].

The first mode corresponds to Tollmien-Schlichting (T-S) waves. The wall cooling, which naturally occurs on hypersonic-vehicle surfaces, strongly stabilizes the first mode, while it destabilizes the second mode. Mack second mode belongs to the family of trapped acoustic waves. Once the second mode sets in, it becomes the dominant instability for all hypersonic boundary layers because its growth rate tends to exceed that of the first mode[1]. And the most amplified second-mode wavelength is approximately twice the boundary-layer thickness, and its phase velocity tends to the boundary-layer edge velocity of mean flow. According to the transition procedure, stabilizations of second mode are critical to transition control at high Mach number conditions.

To damp the second mode instabilities, multiple techniques have been proposed including local porous coatings[3-5], wavy wall[6][7], roughness elements[8] and heating or cooling trips[9]. The second-mode instability can be affected by local shaping of the body surface and boundary layer thickness. Once the boundary layer is changed by an appropriate cavity, the instability of second mode could be reduced. For this reason, the effect of local long shallow cavity on hypersonic boundary layer is analyzed.

In this paper, we discuss the result of direct numerical simulation (DNS) of unsteady two-dimensional hypersonic flow. The Navier–Stokes equations are solved numerically for disturbances generated by a local forcing (periodic suction-blowing) at the free-stream Mach number 6 in the near wall flow with local long cavities. The effect of the cavity on the second mode is analyzed. The influence of depth of the cavities is investigated in this study.

2. Problem Formulation and Numerical Simulation

In this study, the stability of a hypersonic boundary layer over a flat plate to wall blowing-suction with the effect of a long shallow cavity investigated by spatial direct numerical simulation[6][9].

2.1 Numerical Simulation Method

The Navier–Stokes equations for 2D viscous compressible unsteady flows are solved numerically and The dependent variables are normalized to the corresponding free-stream parameters and plate length *L**. Pressure is normalized by doubled dynamic pressure and time *t** is normalized by *L*/u**. The dimensionless conservative form of these equations is

$$\frac{\partial U}{\partial t}+\frac{\partial F_1(U)}{\partial x}+\frac{\partial F_2(U)}{\partial y}=\frac{\partial G_1}{\partial x}+\frac{\partial G_2}{\partial y}, \tag{1}$$

$$U=\begin{bmatrix}\rho\\ \rho u\\ \rho v\\ E\end{bmatrix}, U=\begin{bmatrix}\rho u\\ \rho u^2\\ \rho uv\\ u(E+p)\end{bmatrix}, F_2(U)=\begin{bmatrix}\rho v\\ \rho uv\\ \rho v^2+p\\ v(E+p)\end{bmatrix},$$

$$\tau_i j=\begin{cases}\dfrac{\mu}{Re}(\dfrac{\partial u_i}{\partial x_j}+\dfrac{\partial \mu_j}{\partial x_i}), & i\neq j\\ \dfrac{\mu}{Re}(2\dfrac{\partial u_i}{\partial x_i}+\dfrac{2}{3}divV), & i=j\end{cases} \tag{2}$$

$$p=\frac{1}{\gamma Ma^2}\rho T \tag{3}$$

$$Re=\frac{\rho^* u^* l_\infty^*}{\mu^*},\quad E=\rho(e+\frac{u^2+v^2}{2}),\quad Ma=\frac{u^*}{a^*},\quad (a^{*2}=\gamma R^* T^*) \tag{4}$$

The superscript * denotes dimensional variables and the subscript ∞ denotes flow variables in the freestream. The dynamic viscosity coefficient μ is calculated by applying Sutherlands law. The test gas in the hypersonic flow is assumed a perfect gas with the specific heat ratio γ = 1.4 and Prandtl number *Pr* = 0.72.

The 2-D Navier–Stokes equations are solved numerically by using a high-order finite difference method. The fifth-order upwind scheme is used to discretize inviscid flux derivatives of the governing equations. Meanwhile, a sixth central difference scheme is used for the discretization of viscous terms, and a third-order Runga-Kutta method is used for temporal integration.

2.2 Problem Formulation

In current numerical studies, the problem is simplified as the hypersonic flow traveling along a 2D flat-plate with a cavity at a zero angle of attack, as shown in Figure 1. These conditions are: *Ma* = 6.0, $Re_\infty^* = 10.5\times10^6 m^{-1}$, T_w^* = 293K.

The problem is solved in two steps [6][9]. First, a steady laminar flow field is computed using a time-dependent method. Then, unsteady disturbances are imposed onto the steady solution – a local periodic suction-blowing(as shown in Figure 1) is introduced on the wall via the boundary condition for the mass-flow perturbation:

$$q_w(x,t)=\varepsilon\sin(2\pi\frac{x-x_1}{x_2-x_1})\sin(2\pi f t), \tag{5}$$

where: x_1 = 0.05, and x_2 = 0.075 are boundaries of the suction-blowing region. Where $q_w=\rho_w^* v_w/(\rho_\infty^* v_\infty)$ is dimensionless mass flow in the normal wall direction. A small forcing amplitude ε = 0.001 is adopted to ensure the linear evolution of excited disturbance. The forcing frequency is fixed at f^* = 138.74Hz.which corresponds to the dimensionless frequency parameter $f=f^*L^*/U_\infty^*$ =35.1. This value results in the maximum amplitude of wall pressure perturbation at $x=0.75$.

Synchronization point of F mode and S mode under the flow condition in this study is at $x=0.51$. The local long shallow cavity is located downstream of the synchronization point. The length of the local

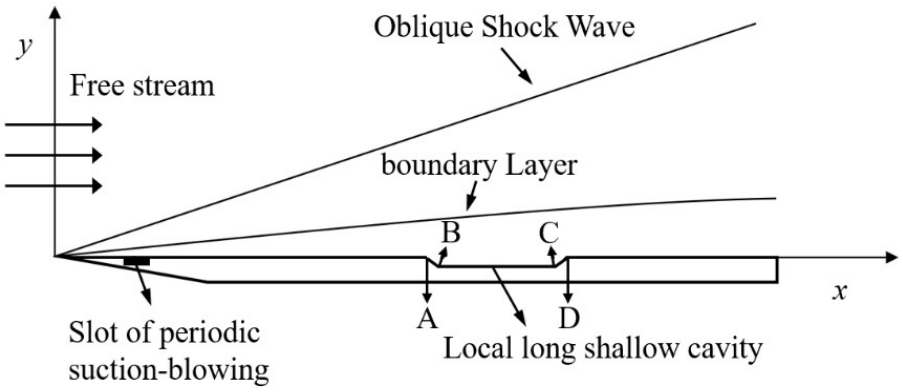

Figure 1 – Schematic drawing of plate with cavity.

long shallow cavity is approximately eight times of local second mode wavelength and the maximum depth is approximately one third of the second mode wavelength. Case0 is flat plate and three cases with different depth of cavities are studied, the coordinate of the points in Figure 1(A, B, C, D) in different cases are shown in table 1. The depth of the cavity in case1 is 0.002, the depth of the cavity in case2 is 0.004 and the depth of the cavity in case3 is 0.008.

Table 1 – Coordinate of the points in different computational case

	A	B	C	D
case1	(0.5, 0)	(0.53, -0.002)	(0.67, -0.002)	(0.7, 0)
case2	(0.5, 0)	(0.53, -0.004)	(0.67, -0.002)	(0.7, 0)
case3	(0.5, 0)	(0.53, -0.008)	(0.67, -0.002)	(0.7, 0)

2.3 Verification

The cases that mack mode developing above a smooth-wall and a porous surface[10][11] (porosity n = 0.25, pore depth d =1 and 8 pores per wavelength) are chosen to validate the accuracy of DNS. The comparison of the instantaneous disturbance fields of calculation result and reference result is shown in Figure 2[10]. The growth rate on porous surface is 51.4% of the smooth-wall case and this value is 51% in reference. Two results are almost identical, which could validate the DNS code applied in this research.

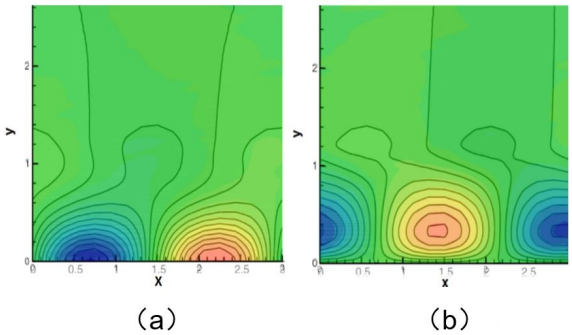

Figure 2 – Disturbance fields on smooth-wall; (a) – pressure, (b) – vertical velocity; color – calculation result, black lines – result in reference.

3. Numerical Result

3.1 Steady Flow

The computed steady-flow pressure field over a flat plate is shown in Figure 3. There is a weak shock wave generated near the flat-plate leading edge due to the viscous-inviscid interaction as seen from the pressure contour. An expansion wave can be observed near the leading edge of the cavity and a compression wave can be observed near the cavity trailing edge induced by the shear layer

impingement. As the streamline near the wall shown in Figure 3, one may conclude that the chosen cavity weakly affects the global flow field over the boundary layer.

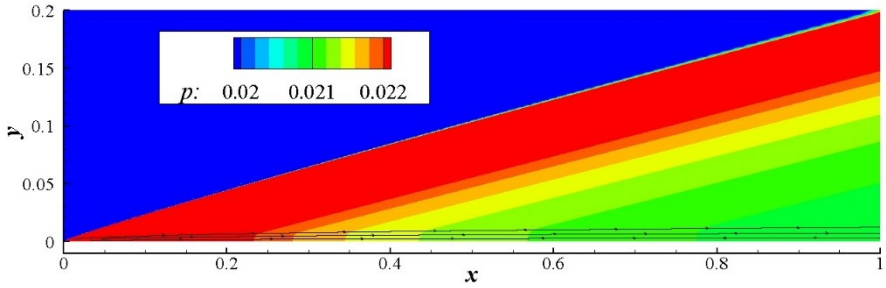

(a) case0

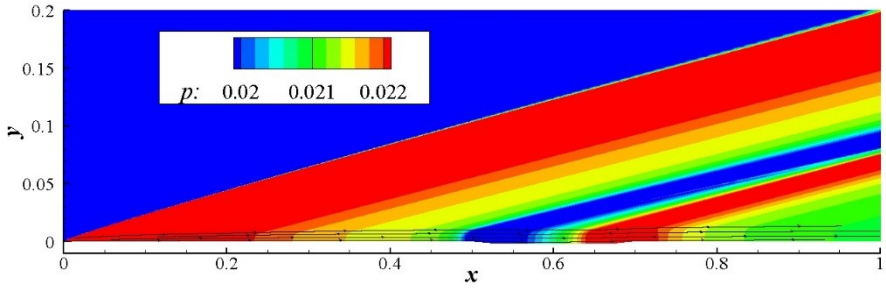

(b) case1

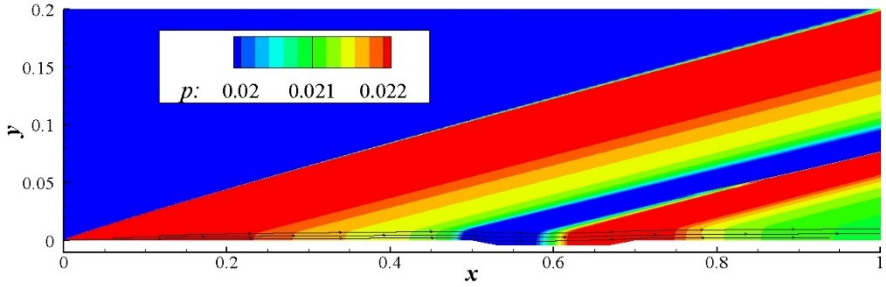

(c) case2

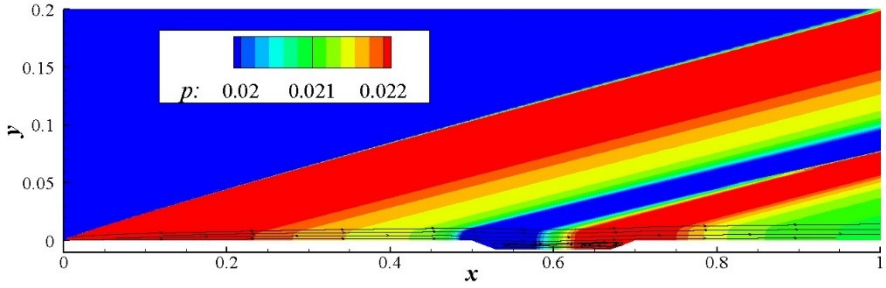

(d) case3

Figure 3 - Pressure field of steady flow.

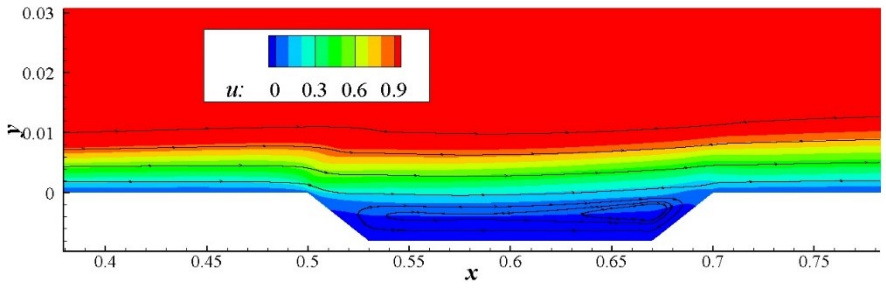

Figure 4 - Horizontal velocity field of steady flow.

The streamwise velocity profiles in the wall-normal direction at different locations show that the flow is

almost unaffected in the upstream region of the cavity. At the location during the streamwise range of cavity, the velocity profile is strongly distorted. Downstream of the cavity, deviation from the baseline results decreases layer and a nonzero velocity and the velocity profile is eventually reestablished. The results indicate that the cavity only has local effects on the steady base flow. For the deepest cavity within the scope of the study(case3), flow separates from the leading edge of the cavity resulting in a shear layer bridging the length of the cavity. And no self-sustaining oscillations occur in the base flow, as seen in Figure 4.

3.2 Unsteady Flow

At first disturbance evolution is computed for a flat plate. In this case, the computational domain is a rectangular of dimensions 1×0.2. The flow parameters and the boundary conditions are the same as in Section II.

A fragment of the instantaneous disturbance field over flat plate (the difference between a disturbed flow field and a steady field) inside the boundary layer is shown in Figure 5. For $x > 0.5$, the boundary-layer disturbance corresponds to the second mode, which is typified by two-cells in the pressure field and rope-like formations in the temperature field.

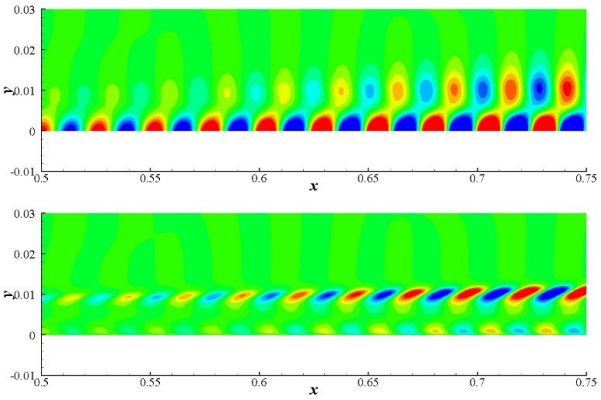

Figure 5 - Fields of pressure (top) and temperature (bottom) disturbances over the flat plate for f = 35.1 in the range of maximum growth rate.

Figure 6 shows the instantaneous fluctuating pressure field over plate in different cases. Perturbation induced by blowing-suction propagates downstream with the phase velocity slightly lower than the velocity at the boundary-layer edge. As trapped acoustics waves, the second-mode waves are reflected between the wall and the sonic line. The evolution of the pressure perturbation is unaffected upstream of the cavity. The evolution of the second mode in the vicinity of the cavity is strongly distorted.

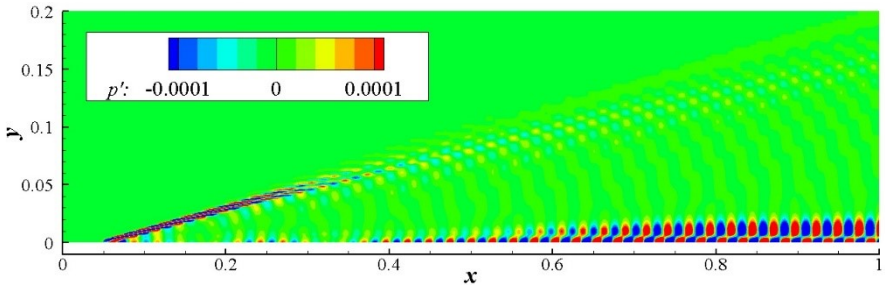

(a) case0

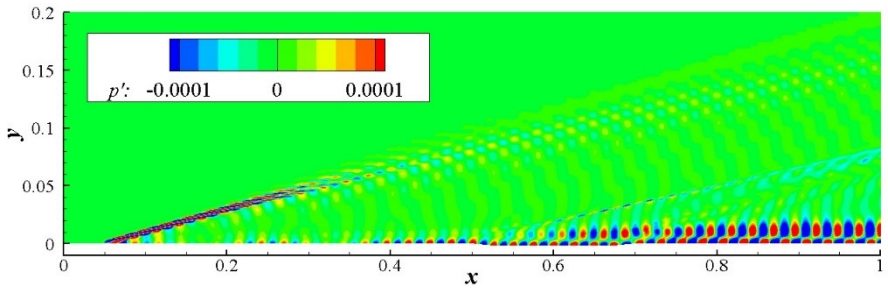

(b) case1

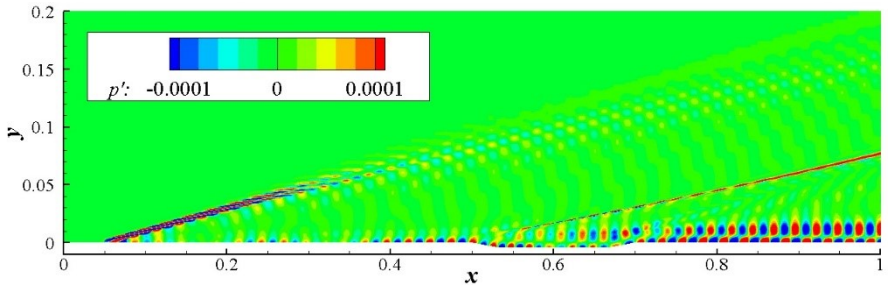

(c) case2

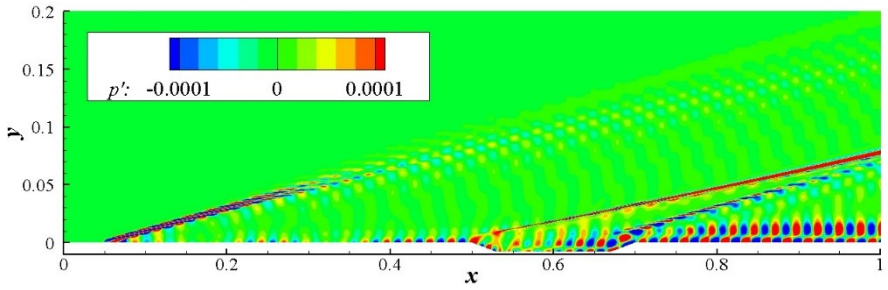

(d) case3

Figure 6 - Instantaneous fluctuating pressure field for different over plate with cavity

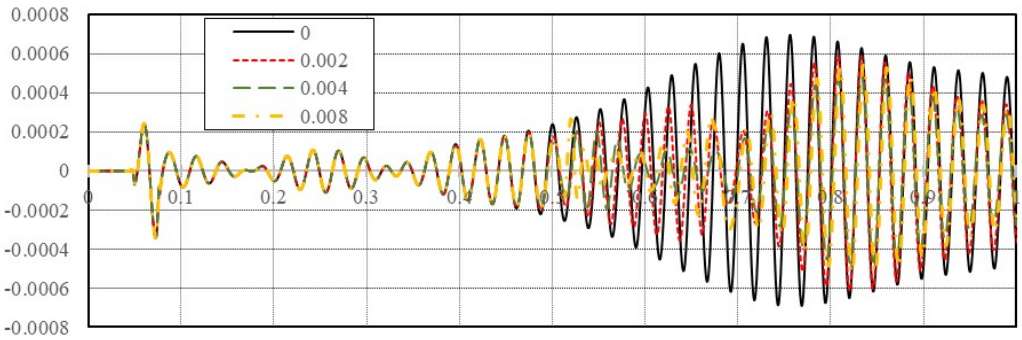

Figure 7 - The wall pressure disturbance for different cases(0:case0, 0.002:case1, 0.004:case2, 0.008:case3,), f = 35.1.

As shown in Figure 7 for the disturbance of fixed frequency f = 35.1, on a flat plate the second mode amplifies and reaches its maximum amplitude at $x \approx 0.75$, while on the plate with cavity the disturbance damps sharply. Compare the pressure perturbation along streamwise along the wall, the amplitude of pressure perturbation reduced significantly. When there is no flow separation in the cavity, the efficiency of damping second mode improves as the depth of the cavity increase (as seen in case1 and case2). As separation flow appears in the cavity, the efficiency of damping second mode instability reduces slightly (as seen in case3).

A local long shallow cavity located in the close downstream region of the synchronization point corresponding to the most dangerous frequency prevents from the intensive second-mode growth in hypersonic boundary layer.

4. Conclusion

Stability of the separated supersonic near-wall flow over plate with cavity is simulated by means of numerical integration of two-dimensional Navier–Stokes equations. It is shown that high-frequency blow-suction effectively excites the second mode in the boundary layer flow. Then the second mode is stabilized over the plate with cavity. The results indicate this is an efficient way to stabilize the second-mode instabilities to put a local cavity in appropriate region. With the depth of the cavity increases, the stabilization of second mode improved. But flow separation in the cavity reduces the stabilization effect.

5. Contact Author Email Address

Yang Jiaji: yangjiaji@buaa.edu.cn

6. Copyright Statement

References

[1] Fedorov A. Transition and stability of high-speed boundary layers. *Annual Review of Fluid Mechanics*, Vol. 43, pp 79-95, 2001.

[2] Egorov. I. V, Fedorov A. and Soudakov V. G. Receptivity of a hypersonic boundary layer over a flat plate with a porous coating *J. Fluid Mech.*, Vol. 601, pp 165-187, 2008.

[3] Malmuth N, Fedorov A, Shalaev V, et al. Problems in high speed flow prediction relevant to control. *2nd Theoretical Fluid Mechanics Meeting*, 2695, 1998.

[4] Fedorov A., Malmuth N., Rasheed A. and Hornung H. G. Stabilization of Hypersonic Boundary Layers by Porous Coatings. *AIAA JOURNAL*, Vol. 39, No. 4, pp 605-614, 2001.

[5] Fedorov A., Shiplyuk A., Maslov A., Sidorenko A. Burov E. and Mulmuth N., Stabilization of a Hypersonic Boundary Layer using an Ultrasonically Absorptive Coating. *J. Fluid Mech.*, Vol. 479, pp 99-124, 2003.

[6] D. Bountin, T. Cchimitov, A. Maslov, et al. Stabilization of a hypersonic boundary layer using a wavy surface. *AIAA JOURNAL*, Vol. 51, pp 1203–1210, 2013.

[7] Egorov I.V., Novikov A.V., Fedorov A.V., Direct numerical simulation of supersonic boundary layer stabilization using grooved wavy surface. *AIAA paper*, AIAA-2010-1245., pp 1-11, 2010.

[8] Fong K.D., Wang X.W., Zhong X.L., Parametric study on stabilization of hypersonic boundary-layer waves using 2-D surface roughness. *AIAA paper*, AIAA-2015-0837, 0837, 2001.

[9] Zhao R, Liu T, Wen C Y, et al. Theoretical modeling and optimization of porous coating for hypersonic laminar flow control. *AIAA JOURNAL*, Vol. 56, No. 6, pp 2942-2946, 2018.

[10] Sandham N. and Ludeke H., Numerical Study of Mach 6 Boundary-Layer Stabilization by Means of a Porous Surface. *AIAA JOURNAL*, Vol. 47, No. 9, pp 2243-2252, 2009.

[11] Tullio N. and Sandham N., Direct Numerical Simulation of Breakdown to Turbulence in A Mach 6 Boundary Layer over A Porous Surface. *Physics of Fluids*, Vol. 22, pp 1-14, 2010.